Innovative Food Science and Emerging Technologies 37 (2016) 125–137

Contents lists available at ScienceDirect

Innovative Food Science and Emerging Technologies

journal homepage: www.elsevier.com/locate/ifset

Computer simulation analyses to improve radio frequency (RF) heating uniformity in dried fruits for insect control

Bandar Alfaifi [a,*], Juming Tang [b], Barbara Rasco [c], Shaojin Wang [d], Shyam Sablani [b]

[a] Department of Agricultural Engineering, King Saud University, P.O. Box 2460, Riyadh 11451, Saudi Arabia
[b] Department of Biological Systems Engineering, Washington State University, Pullman, WA 99164-6120, USA
[c] School of Food Science, Washington State University, Pullman, WA 99164-6376, USA
[d] College of Mechanical and Electronic Engineering, Northwest A&F University, Yangling, Shaanxi 712100, China

ARTICLE INFO

Article history:
Received 14 April 2016
Received in revised form 11 August 2016
Accepted 15 August 2016
Available online 16 August 2016

Keywords:
Computer simulation
Dried fruits
Insect disinfestation
Electrode configuration
Heating uniformity
RF heating

ABSTRACT

In recent years, radio frequency (RF) heating has been explored as a new postharvest pest and pathogen control procedure for agricultural commodities and dry food ingredients. Non-uniform heating and, sometimes runaway heating, have been the major challenges with implementation of this technology. In this study, an experimentally validated computer simulation model was developed to predict the effects of different package geometries, electrode configurations, and use of forced air (60 °C) on improving the heating uniformity of raisins treated with RF for insect control. Higher temperatures (60–76 °C) were observed in the areas between the edges and corners on the top and bottom layers of the RF treated raisins held in rectangular and cylinder shaped containers, with lower temperatures (40–52 °C) observed in the central areas of each layer. The heating uniformity was improved by rounding the corners of the containers and reducing sharp edges on the packages, modifying electrode configurations, and applying forced air after RF heating. These modifications reduced the maximum temperature difference throughout a container of heated raisins to about 5 °C. Approximately 356 min were needed to raise the raisin temperature in a rectangular container from 23 °C to 55–60 °C using only forced air at 60 °C. In contrast, only 6 min of RF heating followed by 10 min of forced air treatment at 60 °C was needed for a similar filled container to reach a temperature of 55–60 °C. Shortening the electrodes length to 4 cm shorter than the horizontal dimensions of the rectangular containers also improved heating uniformity. This technique can be easily implemented to improve the uniformity of RF heating in the food industry for the control of insects in packaged dried fruits.

Industrial relevance: The results in this study provide essential information about the non-uniform heating inside the RF heated materials packed in containers with sharp areas, edges and corners, such as rectangular and cylindrical shaped containers. Rounding the edges and corners in the containers or bending the top and bottom electrodes is key parameters to control the electrical field inside the RF system. This technique can be easily implemented to improve the uniformity of RF heating in the food industry for the control of insects in packaged dried fruits.

1. Introduction

Radio frequency (RF) heating involves heating with electromagnetic waves (3 kHz to 300 MHz) (Ramaswamy & Tang, 2008) and to avoid interference with other communication systems, only three frequencies, 13.56, 27.12, and 40.68 MHz, are allocated for industrial, medical, and scientific applications in the USA (Wang et al., 2001). RF, like microwave, is a form of volumetric heating and provides opportunities for rapid heat treatments to control pests and pathogens in bulk materials. However, several challenges still exist that limit successful commercialization of these RF applications with the most important challenge being uneven temperature distribution (Fu, 2004). Various factors influence RF heating uniformity, including the dielectric, thermal and other physical properties, as well as the position of the treated product relative to electrodes, the chemical and physical properties of the surrounding medium and the engineering design of the treatment system (Fu, 2004). Severe uneven heating can cause both package and product damage. Several studies have explored RF as a non-chemical alternative for insect disinfection in agricultural commodities and for thermal treatments for pathogen control in bulk dry food ingredients, starting with the early work of Lutz (1927); Headlee and Burdette (1929), and Hadjinicolaou (1931) proceeding to more current research of Huang, Zhang, Marra, & Wang (2016); Jeong and Kang (2014); Ha, Kim, Ryu, and Kang (2013), and Jiao, Johnson, Tang, and Wang (2012). Solving the problem of non-uniform heating in RF heated low and intermediate

* Corresponding author at: P.O. Box 2460, Riyadh 11451, Saudi Arabia.
E-mail address: balfaifi@ksu.edu.sa (B. Alfaifi).

http://dx.doi.org/10.1016/j.ifset.2016.08.012
1466-8564/

Nomenclature

V	electric potential, V
E	electric field strength, V m^{-1}
C_P	specific heat, J kg^{-1} K^{-1}
f	frequency, Hz
k	thermal conductivity, W m^{-1} K^{-1}
Q	power dissipation, W m^{-3}
t	time, s
T	temperature, °C
$T_{initial}$	initial temperature, °C
T_{av}	average temperature, °C
V_{vol}	material volume, m^3
UI	uniformity index

Greek symbols

ε	complex relative permittivity, F m^{-1}
ε_0	permittivity of free space, F m^{-1}
ε'	dielectric constant
ε''	dielectric loss factor
σ	electrical conductivity, S m^{-1}
∇	vector differential operator
ρ	density, kg m^{-3}

Subscripts

0	free space
av	average
vol	volume

moisture foods is critical if effective thermal treatments are to be developed.

A number of methods have been suggested to improve RF heating uniformity including: modifying the composition of the media (e.g. saline water, hot water, or air) surrounding the product (Ikediala, Hansen, Tang, Drake, & Wang, 2002; Birla, Wang, Tang, & Hallman, 2004; Wang, Tiwari, Jiao, Johnson, & Tang, 2010; Harraz, 2007), rotation (Birla et al., 2004), mixing, back and forth agitation of the product containers between two plate electrodes (Wang et al., 2010; Ling, Hou, Li, & Wang, 2016), and cycling of the power (pulse mode) (Hansen et al., 2006). Recently, Zhou, Ling, Zheng, Zhang, and Wang (2015) and Zhou and Wang (2016) developed an effective RF treatment protocol based upon a laboratory-scale RF system to control *S. oryzae* in rough, brown, and milled rice. Heating uniformity was improved by enhancing the RF treatment with hot air circulation, mixing, and back and forth movement of the product container while maintaining acceptable product quality. Combining a fruit conveyer with hot water surface disinfestation treatment in RF systems improved heating uniformity in oranges (Birla et al., 2004), apples (Wang, Birla, Tang, & Hansen, 2006), persimmons (Tiwari, Wang, Birla, & Tang, 2008). Sosa-Morales et al. (2009) improved RF heating uniformity of mangoes by combining hot water heating with RF heating while rotating the fruits in a fruit mover for the purpose of controlling Mexican fruit fly. Pre-heating the fruits in water at 45 °C for 50 min, followed by RF heating in a 27.12 MHz, 12 kW RF system for 1 min to reach 48 °C, and holding in water at 48 °C for 6 or 8 min, should meet the disinfestation requirements of mangoes without destroying the fruits quality.

To reduce the time and development cost associated with extensive trial and error experimentation to improve heating uniformity of RF processes, computer simulations can be useful for predicting essential information to facilitate the design and scale-up and to explore operational parameters. Several simulation models have been developed to study different factors and methods for improving RF heating uniformity for different food materials, such as oranges (Birla, Wang, & Tang, 2008), wheat flour (Tiwari, Wang, Tang, & Birla, 2011b; Tiwari, Wang, Tang, & Birla, 2011a), wheat kernel (Chen, Wang, Li, & Wang, 2015), peanut butter (Jiao, Tang, & Wang, 2014), meat (Uyar et al., 2015), and soybeans (Huang, Zhang, Marra, & Wang, 2016). Marra, Lyng, Romano, and McKenna (2007) studied temperature distributions in RF heating of meat batters in cylindrical molds at different output powers and heating rates solving electromagnetic and heat equations using the finite element analysis (FEMLAB) finding that lower output power resulted in more even temperature distributions. About 70% of the time experimental and predicted temperatures for the meat batters agreed with an uncertainty of 2.2 °C. Birla et al. (2008) used a validated finite element-computer simulation analysis (FEMLAB) to solve coupled Maxwell's EM equations and Navier–Stokes equations; they further studied the effect of dielectric properties of fruit (orange) and the surrounding heating medium, and rotation of the fruit in the EM field on heating uniformity and predicted insect lethality. Their study demonstrated that the heating uniformity improved by modifying the dielectric properties of the surrounding medium to match that of the fruit and by rotating the fruits in the RF treatment chamber. Tiwari et al. (2011a) employed a finite element model to explore the effects of sample size, shape, position, and dielectric properties of wheat flour and the surrounding medium, electrode gap, and top electrode configuration on the RF power uniformity in wheat flour placed into a 12 kW, 27.12 MHz parallel plate RF system and showed that these factors significantly affected the RF power distribution in RF treated flour. Huang, Marra, & Wang (2016) developed a computer simulation model using a finite element-based commercial software and validated using experimental of

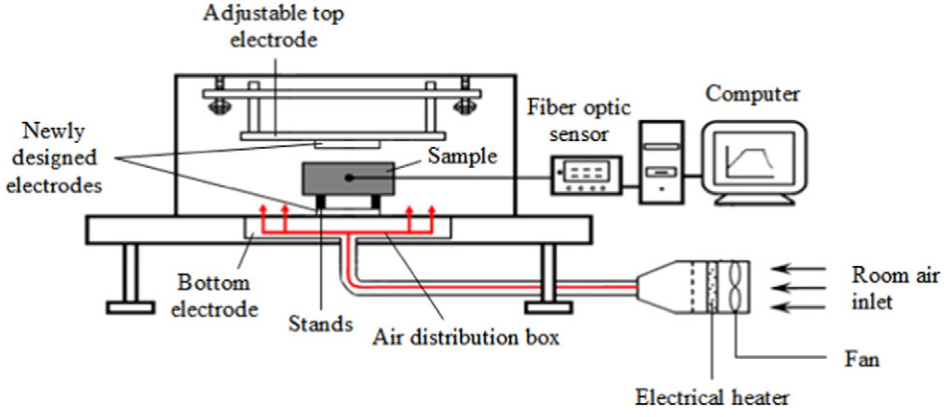

Fig. 1. Schematic view of the pilot-scale 6 kW, 27.12 MHz RF unit showing the rectangular plastic container placed in between the top and bottom electrodes. Adapted from Wang et al. (2010).

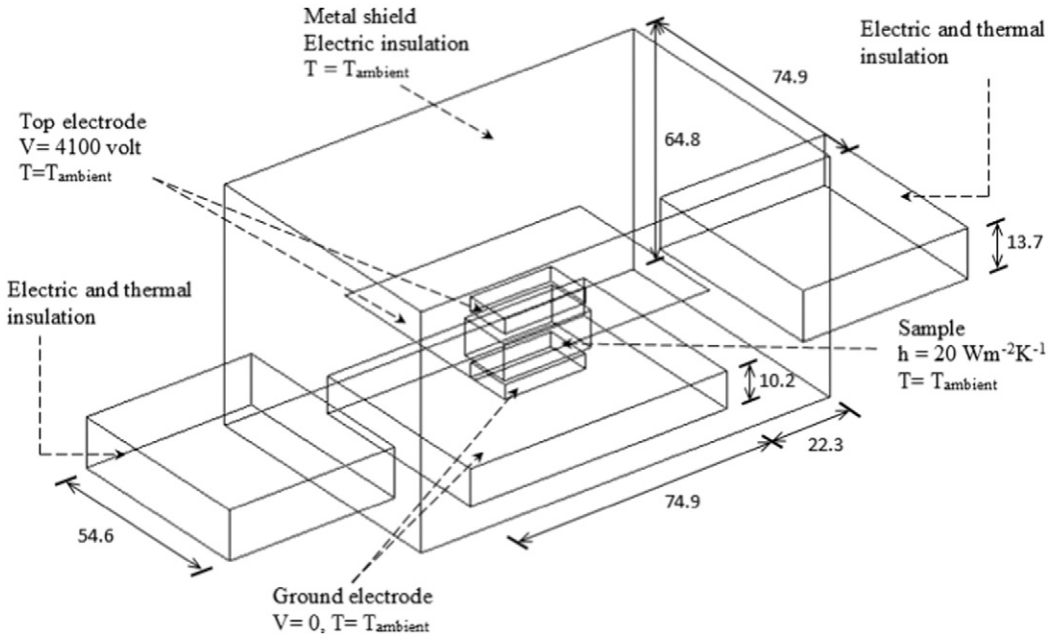

Fig. 2. Geometrical, thermal, and electrical boundary conditions of the 6 kW, 27.12 MHz RF system considered in simulation (all dimensions are in cm).

soybean flour packed in a rectangular container and heated in a 6 kW, 27.12 MHz RF system. The validated model was further used to study the effects of dielectric properties and density of sample and surrounding container on sample RF heating uniformity. Regression equations based on the relationship between these factors were established to assist in selecting the most appropriate surrounding material to improve the RF heating uniformity in various food products and for designing an RF treatment protocol.

Unanswered questions remain regarding the behavior of foods during RF treatment and system designs (e.g. electrode configurations) that result in non-uniform heating. This study addresses overheating that occurs at sharp corners and faces that reduce the effectiveness of post-harvest disinfestation treatment for dried fruits and result in lower food quality. The objectives of this study were for using a validated computer simulation model to evaluate the effects of: 1) package geometry, 2) electrode configuration, and 3) use of forced air (60 °C) on the heating uniformity and heating rate of raisins during RF thermal disinfestations.

2. Materials and methods

2.1. RF and hot air systems as a physical model

A free-running oscillating 6 kW, 27.12 MHz parallel plate RF heating system (COMBI 6-S, Strayfield International Limited, Wokingham, UK), along with a hot air circulation system comprised of a 5.6 kW electrical strip heater and a blower fan, were used to heat the raisins. The RF system has a pair of parallel electrodes (68.6 L × 49.5 W cm^2) in which the top electrode is movable to adjust RF power. Fig. 1 shows a schematic of the RF and hot air systems used in this study. More details about the system can be found in Wang et al. (2010).

Table 1
Dielectric (@ 27.12 MHz), thermal, and physical properties of materials used in computer simulation.

Materials properties	Raisins*	Aluminum**	Air**
Thermal conductivity (k, W m^{-1} $°C^{-1}$)	0.001*T + 0.145	160	0.025
Density (ρ, kg m^{-3})	784	2700	1.2
Specific heat (C_p, J kg^{-1} $°C^{-1}$)	10.9*T + 1831	900	1200
Dielectric constant (ε')	0.081*T + 6.31	1	1
Loss factor (ε'')	0.018*T + 1.88	0	0

Source: *Alfaifi et al. (2013); Alfaifi et al. (2014); **COMSOL material library (2012); ***T is temperature in °C.

2.2. Mathematical model

A computer simulation model developed using a finite element–based commercial software, COMSOL, and validated using experimental data in Alfaifi et al. (2014), was used in this study. The maximum average temperature difference between simulated and experimental data in three horizontal layers of a rectangular plastic container (25.5 L × 15.0 W × 10.0 H cm^3) was about 4 °C (Alfaifi et al., 2014).

2.2.1. Governing equations

For the electric current model, Maxwell's electromagnetic field equations were solved using a quasi-static approximation, this is appropriate since the wavelength (11 m) in the 27.12 MHz RF system is much

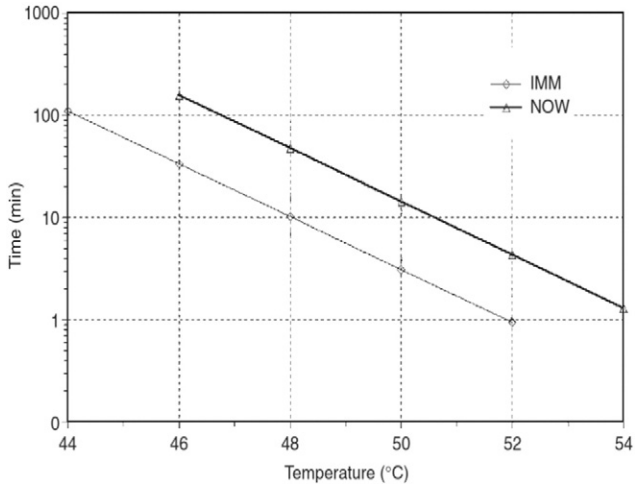

Fig. 3. Minimum time–temperature combinations for complete kill of 600 fifth-instars of Indianmeal moth (IMM) and navel orangeworm (NOW).
Adapted from Wang et al. (2007).

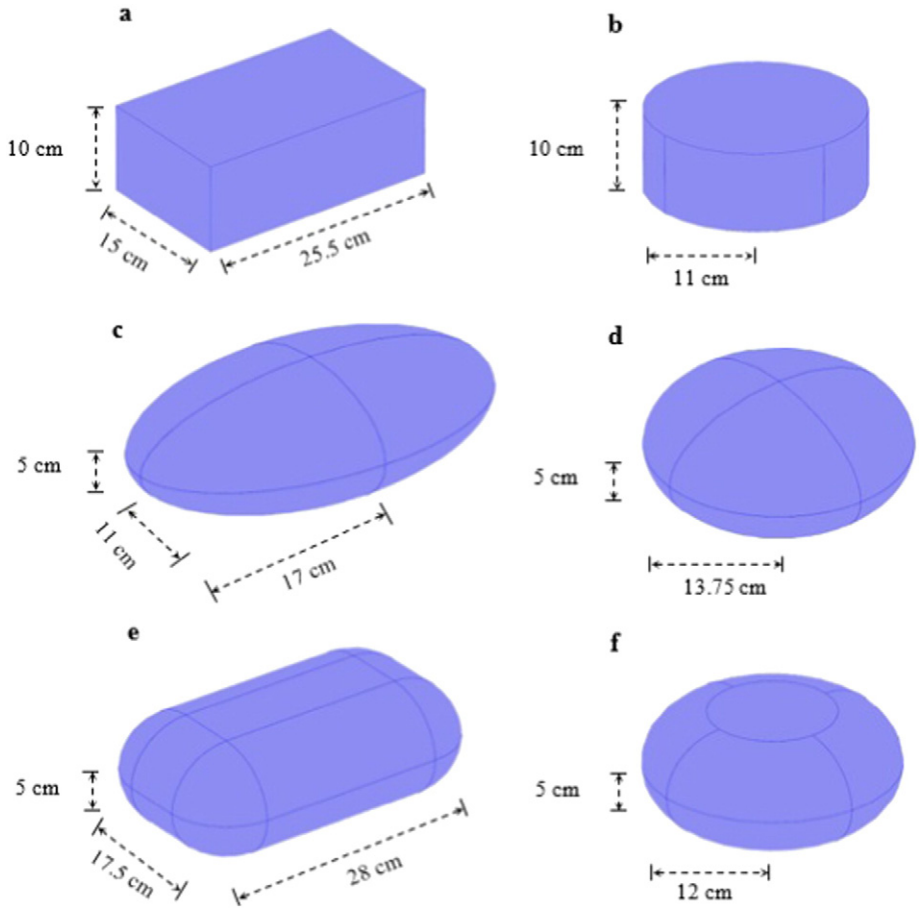

Fig. 4. Sample shapes, a) rectangular (Rec), b) cylinder (Cyl), c) ellipsoid 1 (Ell 1), d) ellipsoid 2 (Ell 2), e) rounded rectangular (RR), and f) rounded cylinder (RC), used in simulation.

higher than the electrode size ($68.6 \times 49.5\ cm^2$) used in this study. The Laplace form of Maxwell's equations is expressed as (Metaxas, 1996):

$$\nabla \cdot ((\sigma + j2\pi f \varepsilon_0 \varepsilon)\nabla V) = 0 \quad (1)$$

where σ is the electrical conductivity ($S\ m^{-1}$), $j = \sqrt{-1}$, f is the frequency (Hz), ε_o is the permittivity of free space ($8.86 \times 10^{12}\ F\ m^{-1}$), ε is the complex relative permittivity of the material, and V is the voltage between the two electrodes (V). The electric field strength is ($E = -\nabla V$). The complex relative permittivity (ε) can be expressed in terms of the relative (to air) dielectric constant (ε') and the relative loss factor (ε'') of the material ($\varepsilon = \varepsilon' - j^*\varepsilon''$).

The heat transfer due to conduction was considered within the food product sandwiched between the electrodes. The governing heat transfer equation is:

$$\rho C_P \frac{\partial T}{\partial t} = \nabla(k\nabla T) + Q \quad (2)$$

where ρ is the density ($kg\ m^{-3}$), C_p is the specific heat ($J\ kg^{-1}\ °C^{-1}$), T is the temperature within the sample (°C), t is the process time (s), k is

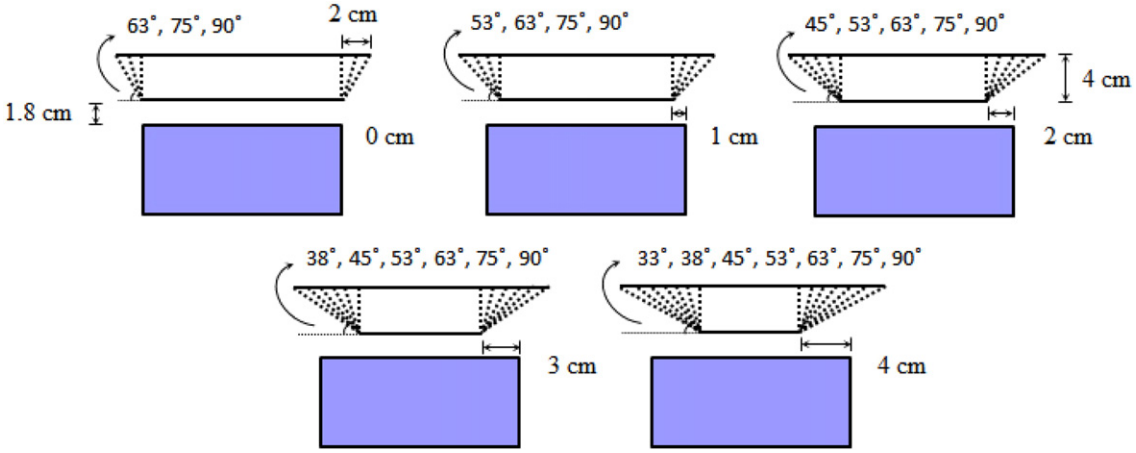

Fig. 5. Rectangular sample with different electrode configurations (similar configurations were applied to the newly designed bottom electrode).

thermal conductivity (W m^{-1} K^{-1}), and Q is the RF power dissipation (W m^{-3}) and is expressed as (Barber, 1983):

$$Q = 2\pi f \varepsilon_0 \varepsilon'' \left|\vec{E}\right|^2 \quad (3)$$

2.2.2. Boundary conditions

Fig. 2 shows the geometrical, thermal, and electrical boundary conditions of the RF system considered in the simulation. Electrical insulation ($\nabla \cdot E = 0$) and thermal insulation ($\nabla T = 0$) were used for the inlet and outlet of the system, while the electrical insulation ($\nabla \cdot E = 0$) was only used for the metal walls of the RF cavity. The bottom electrode was grounded ($V = 0$). A constant electrical voltage (4100 V) was used for the top electrode (Alfaifi et al., 2014). The convective heat transfer ($h = 20$ W m^{-2} K^{-1}) was used for all of the surfaces of the sample (Wang et al., 2001). A uniform initial temperature ($T_{initial} = 23$ °C) was assigned to the sample. A uniform voltage distribution was assumed because 30% of the RF wavelength of 27.12 MHz (11 m) is larger than the dimension of the top electrode (68.6 × 49.5 cm^2) in the RF system (Metaxas, 1996). Steady voltage was assumed in the operating RF system as it differs by only 7% in

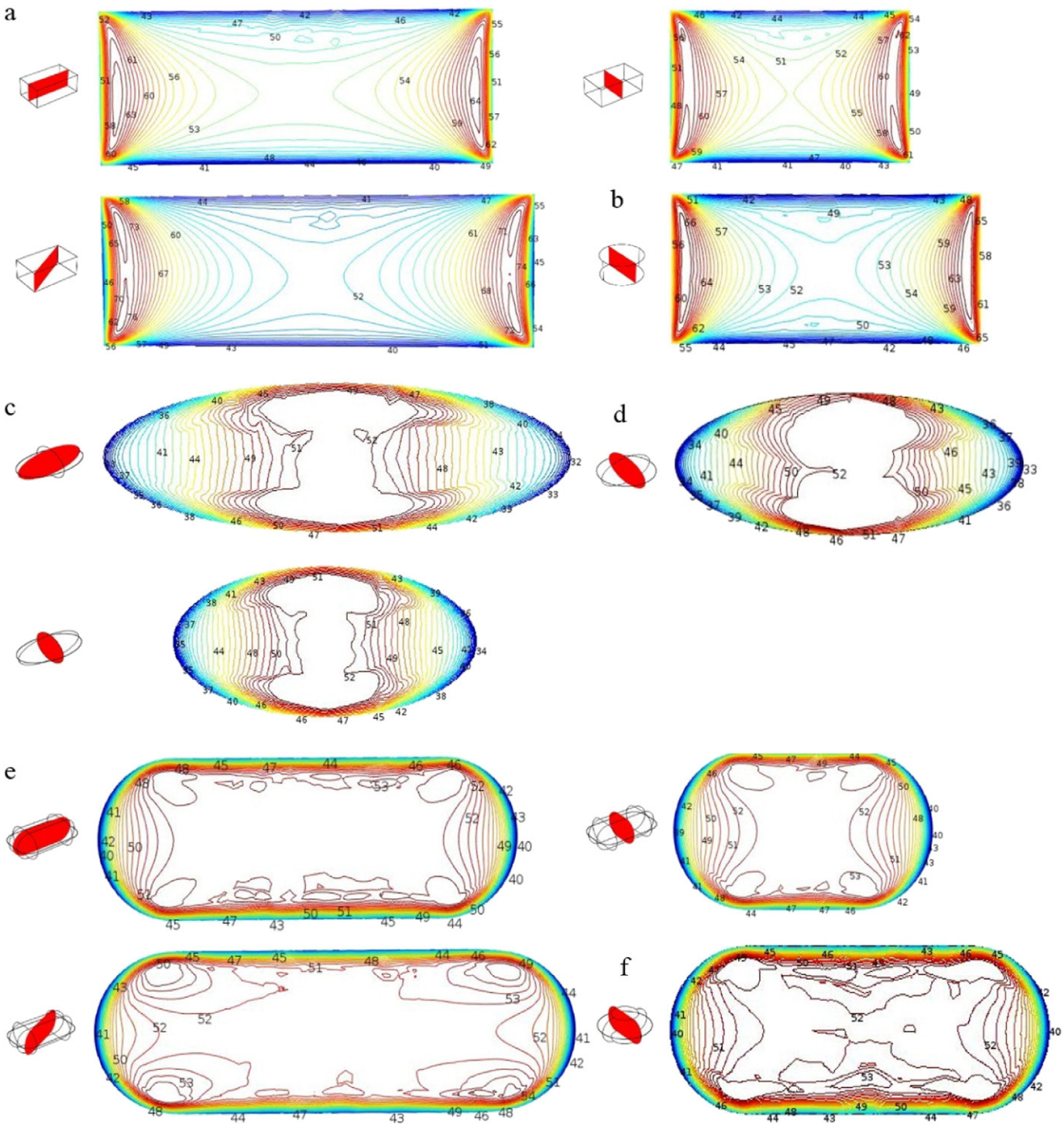

Fig. 6. Temperature distributions in vertical layers of raisin samples in a) rectangular, b) cylinder, c) ellipsoid 1, d) ellipsoid 2, e) RR, and f) RC shapes and heated to a center temperature of 52 °C using the 6 kW, 27.12 MHz RF system with flat electrodes, gap of 13.6 cm, and initial temperature 23 °C (color scale is set individually for each condition).

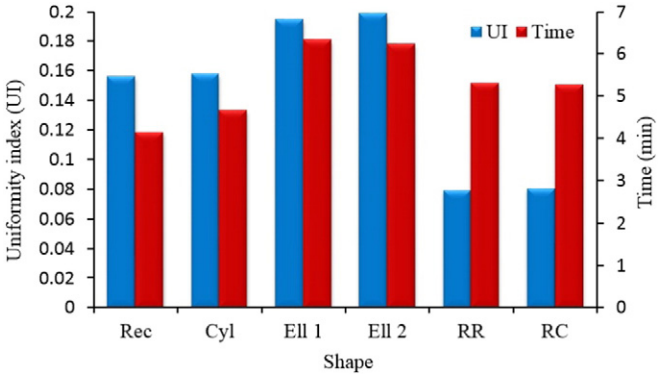

Fig. 7. Effect of sample shape on UI (Uniformity Index) and treatment time of raisins heated to a center temperature of 52 °C using the 6 kW, 27.12 MHz RF system with flat electrodes, gap of 13.6 cm, and initial temperature 23 °C.

typical industrial-scale RF systems between the standby and full load positions (Metaxas, 1996).

During the use of forced air at 60 °C, all of the sample interfaces were assigned to a convective heat transfer boundary condition. To estimate the convective heat transfer coefficient (h) at this condition, several preliminary simulation runs were conducted with different values of h. By comparing the preliminary simulated and experimental central temperatures of the heated raisins, the value of h was estimated to be 54 W m^{-2} K^{-1} as an average for all of the outer surfaces exposed to forced (0.7 m/s) air at 60 °C.

2.2.3. Solution methodology and model inputs

The COMSOL software package (V4.2a, COMSOL Multiphysics, Burlington, MA, USA), based on a finite element method, was used. A US Micro Mini-Tower Workstation with a Core i7-2600, 3.4 GHz Quad Core Processor, and 16 GB RAM running on a Windows 7 64-bit operating system was used to run the software. The Joule heating model, which coupled electric current and heat transfer models, was used. In each simulation sequence, the geometry was first created and a relatively fine mesh was generated at the interface of the sample and the surrounding medium for the finite element models. The mesh system was used after confirming that the final solutions were independent of grid size, meaning that the solution should not change (<0.1%) if the mesh size was further refined. The direct linear system solver, UMFPACK, was used with a relative tolerance and an absolute tolerance of 0.01 and 0.001, respectively. The initial and maximum time steps were set as 0.001 and 1 s. Total solution time for each simulation run varied between 20 and 40 min, depending on the simulation sequence.

The dielectric, thermal, and physical properties of the sample were adapted from Alfaifi et al. (2013) and Alfaifi et al. (2014) and are listed in Table 1. The gap between the electrodes was set to 13.6 cm to heat the sample center from 23 °C to 52–55 °C at a heating rate of 5–10 °C/min. This setting is an appropriate choice for industrial use to completely kill the navel orange worm and Indian meal moth, two pests that could affect raisins (Fig. 3) (Wang, Tang, & Hansen, 2007).

2.3. Simulation sequences

Simulation runs were designed to determine the overheating that commonly occurs in sharp areas, corners and edges, in the rectangular (Alfaifi et al., 2014; Tiwari et al., 2011b) and cylinder shape samples (Birla et al., 2008).

2.3.1. Package geometry

Six package geometries: rectangular-Rec (25.5 L × 15.0 W × 10.0 H cm^3); cylinder-Cyl (11 r × 10 H cm); ellipsoid 1-Ell 1 (5 a × 11 b × 17 c cm^3); ellipsoid 2-Ell 2 (5 a × 13.75 b × 13.75 c cm^3); rounded rectangular-RR (28.0 L × 17.5 W × 10.0 H cm^3 and rounded edges 5 r cm); and rounded cylinder-RC (12 r × 10 H cm and rounded edges 5 r cm), were used to investigate the effects of the sample geometry on the temperature distribution, heating uniformity, and heating rate when heating raisins by RF heating (with flat electrodes) to a central temperature of 52 °C. The parameters of the rectangular geometry were selected based upon the available published results of parameters, length and width, that resulted in highest Power Uniformity Index (worst uniformity heating, the most difficult scenario) for a dielectric material packed in rectangular geometry and heated under the same RF system (Tiwari et al., 2011a). The parameters of other geometries were selected to match the volume of the rectangular geometry, 0.0038 m^3. These geometries, along with their dimensions, are listed in Fig. 4. For the temperature distributions, three vertical layers were considered in the rectangular and rounded rectangular geometries, two vertical layers in the ellipsoid 1 geometry, and one vertical layer in all other package geometries.

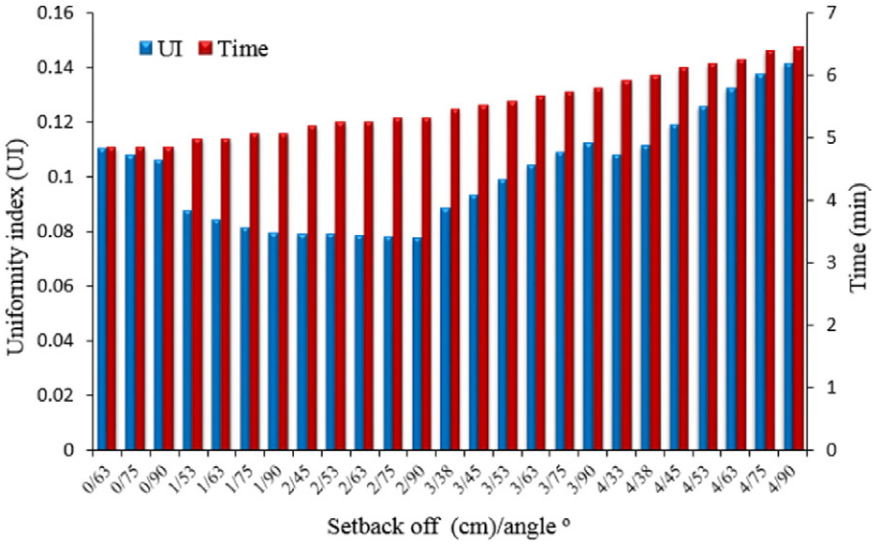

Fig. 8. Effect of different electrode configuration (setback distance and bend angle) on the UI and treatment time of the sample packed in a rectangular shape and heated to a center temperature of 52 °C using the RF system with an electrode gap of 13.6 cm, initial temperature 23 °C, and a constant thickness 4 cm of the newly designed electrodes.

2.3.2. Electrode configuration

Two newly designed electrodes were attached to the flat top and bottom electrodes to study the effect of different combinations of the setback distances (distance between the edge of the sample and the bottom base and the top of the new electrodes), 0, 1, 2, 3, and 4 cm, and bend angles, 90°, 73°, 63°, 53°, 45°, and 33° on the temperature distribution, heating uniformity, and heating rate of raisins packed in a rectangular shaped container following RF heating to a central temperature of 52 °C. A constant thickness, 4 cm, was used in the newly designed electrodes. These configurations were applied to both the new top and bottom electrodes and to all sides. Fig. 5 shows these different configurations. Three vertical layers in the rectangular shape were considered for temperature distribution analyses.

2.3.3. Use of forced air (60 °C) to improve heating uniformity

Due to the lower temperature values observed in preliminary simulations on the outer surfaces of the RF heated raisins compared to the interior area, forced air (60 °C) was used to heat the outer surfaces of the samples. The temperature of the forced air was set to 60 °C and at velocity of 0.7 m/s to shorten the time needed to increase the outer surfaces temperature to 55–60 °C. This time was minimized to preserve the quality of the fruit.

Temperature simulations using forced air at 60 °C were conducted for the electrode configurations that showed the best heating uniformity. The raisins were heated to temperature of 55–60 °C, previously determined to be a safe quarantine level (Fig. 3) and the capability of the electrode configurations for heating to higher central temperatures

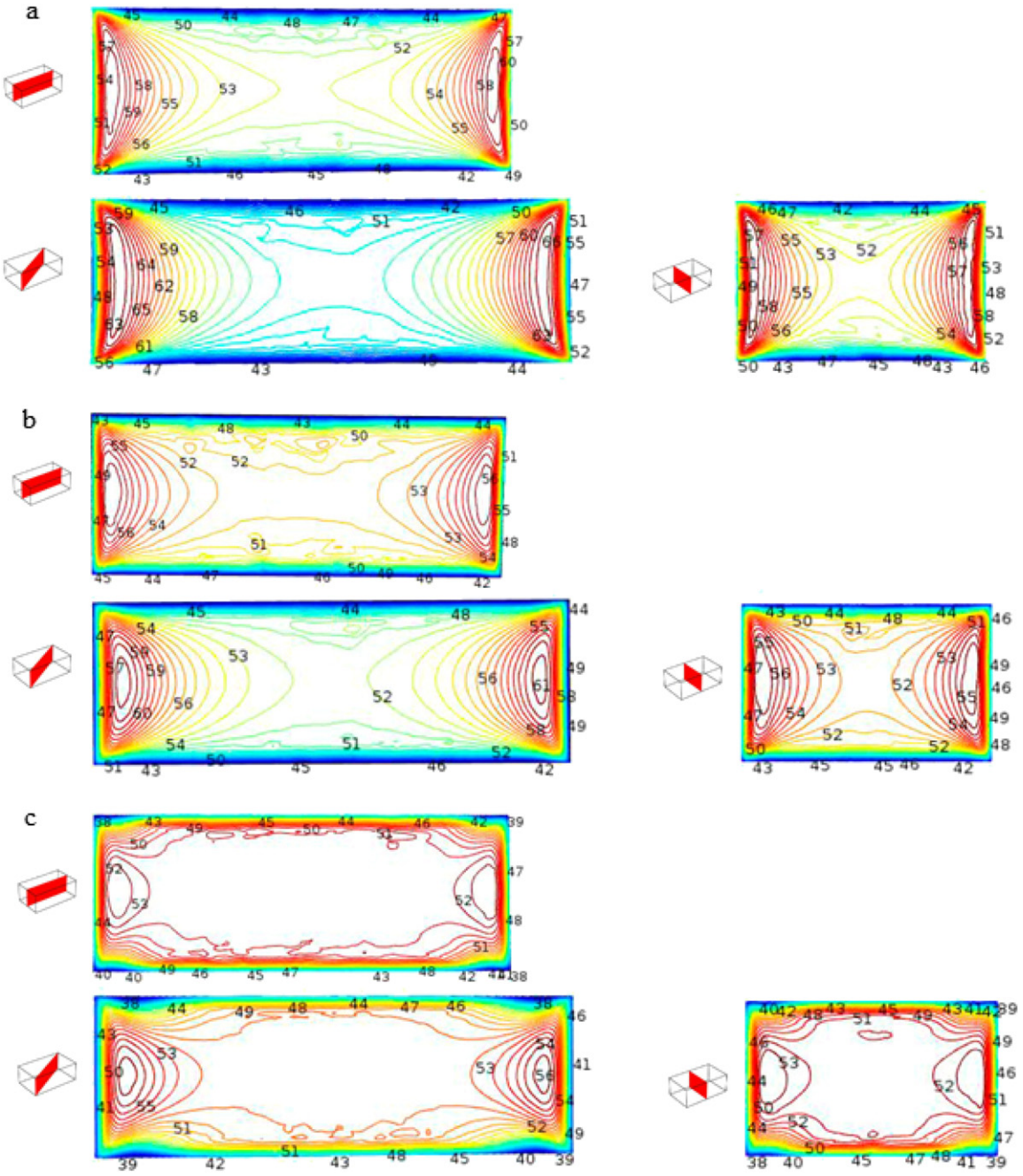

Fig. 9. Effect of different setback distances, a) 0, b) 1 cm, c) 2 cm, d) 3 cm, and e) 4 cm, of the newly designed electrodes (bend angle 90° and thickness 4 cm) on the temperature distributions at three vertical layers of raisin sample in a rectangular shape after RF heating to a center temperature 52 °C with an electrode gap of 13.6 cm and initial temperature 23 °C (color scale is set individually for each condition).

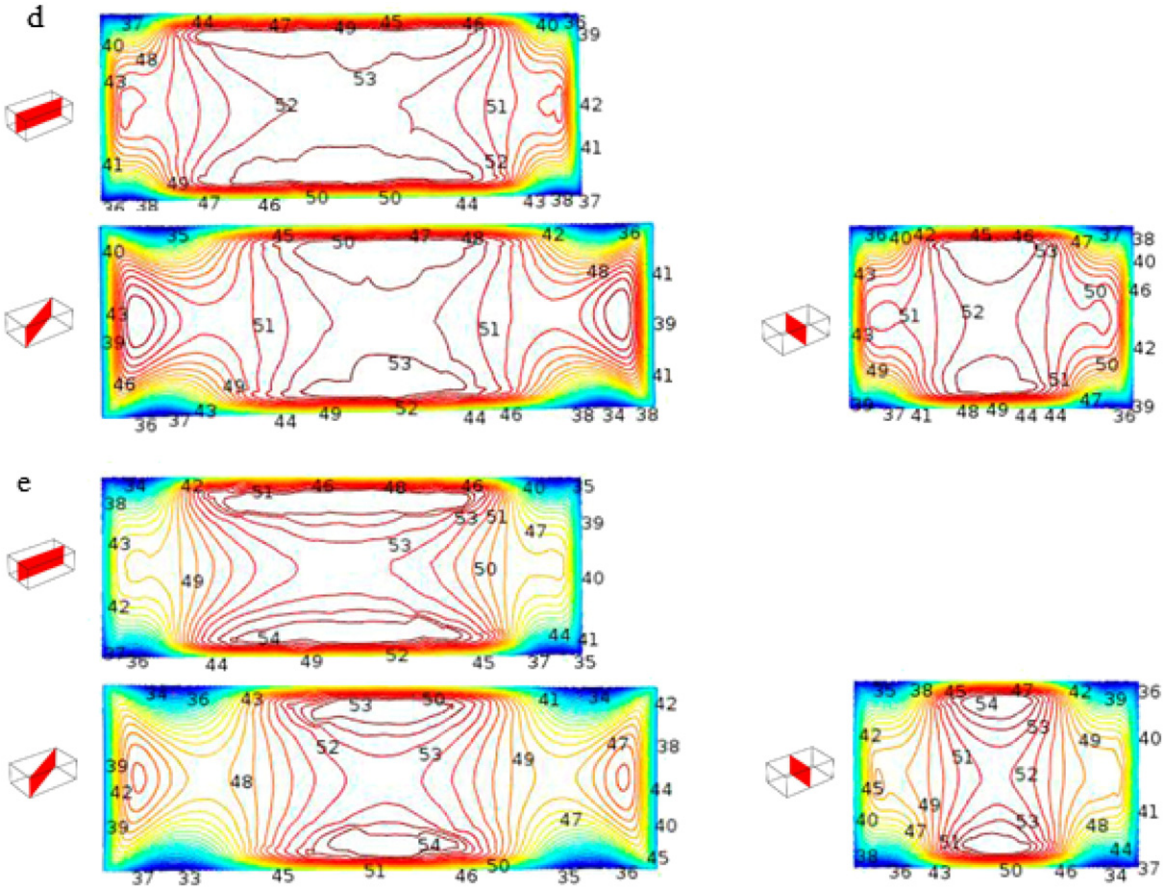

Fig. 9 (*continued*).

with acceptable heating uniformity predicted. Treatment conditions were: forced air (60 °C) heating alone, forced air (60 °C–10 min) followed by RF heating (to a central temperature of 55 °C), simultaneous RF heating and forced air (60 °C) heating, and RF heating (to a central temperature of 55 °C) followed by forced air (60 °C) heating (to outer surfaces temperature of 55–60 °C). From preliminary simulations, after RF heating to a central temperature of 55 °C, about 10 min were needed to raise outer surfaces temperature of the raisins to 55–60 °C using forced air (60 °C), therefore, 10 min of forced air (60 °C) was followed by RF heating condition. Three vertical layers were considered for temperature distribution analyses. The heating uniformity in all of the simulation sequences was evaluated using the uniformity index (UI):

$$UI = \frac{\frac{1}{V_{vol}} \int_{V_{vol}} \sqrt{(T - T_{av})^2} dV_{vol}}{T_{av} - T_{\text{initial}}} \quad (4)$$

where V_{vol} is the material volume (m^3), and T and T_{av} are the local and average temperatures (°C) inside the dielectric material over the volume. The smaller the UI value, the better the RF heating uniformity. A zero value of UI indicates a uniform temperature within a dielectric material.

3. Results and discussion

3.1. Simulation sequences

3.1.1. Package geometry

Simulated temperature distributions in different vertical layers of raisins packed in different geometries and treated in the RF system (with flat electrodes-gap 13.6 cm) to a central temperature of 52 °C are shown in Fig. 6. Higher temperatures (62–64 and 76 °C) were observed in the areas between the edges and corners of the top and bottom layers of the rectangular and cylinder shapes, respectively, when compared to the lower temperatures (40 °C) in the middle flat areas of both sample shapes (Fig. 6a and b). Similar behavior was observed for wheat flour when heated in shapes with sharp areas (Tiwari et al., 2011a; Tiwari et al., 2011b). Electromagnetic field lines between the top and bottom electrodes of the RF systems are straight without a load. However, when a dielectric loss material is placed between the two electrodes, the electromagnetic field lines will attempt to bend and enter the dielectric loss material in one direction at the flat areas. In sharp areas, like the edges and corners in a rectangular shape, more electromagnetic field lines will converge from two or three directions from different faces, causing higher localized temperature zones (Datta & Zhang, 2001). When using the ellipsoid 1 and 2 shapes, which do not have sharp areas, the temperatures (32–34 °C) of the outer side surfaces were reduced when compared to that of the sample shapes with the sharp areas (Fig. 6c and d). However, higher temperatures (52 °C) were observed in the central areas of these shapes when compared to the outer side surfaces. Rectangular and cylinder shapes with rounded edges and corners showed more uniform temperature distributions when compared to other tested shapes, as shown in Fig. 6e and f. It is clear that with reduced sharp areas in these shapes, the electromagnetic field lines enter the rounded edges and corners from one direction, rather than multiple directions, as is the case with sharp areas in the regular rectangular and cylinder shapes. As a result, the electromagnetic field concentration at the rounded edges and corners was reduced.

Fig. 7 compares the UI and time needed to raise the central temperature from 23 °C to 52 °C in the studied sample shapes. The UI was low, indicating uniform temperature distribution, for sample shapes with

reduced sharp areas, the rounded rectangular and cylinder shapes. The UI was reduced from 0.16–0.2 for the rectangular, cylindrical, ellipsoid 1, and ellipsoid 2 shapes to 0.08 for both the rounded rectangular and rounded cylindrical shapes. The resulted high UIs for the rectangular, cylindrical shapes were due to overheating in the areas between the edges and corners of the top and bottom layers and the lower temperatures in the outer side surfaces of ellipsoid 1, and ellipsoid 2 shapes. About 4 and 4.5 min were needed to increase the central temperature from 23 to 52 °C when heating the raisin sample in the rectangular and cylinder shapes, respectively. For shapes with reduced sharp areas, such as in ellipsoid 1 and 2, the required time increased to about 6 min. The time required for the rounded rectangular and cylinder shapes was about 5 min.

3.1.2. Electrodes configuration

Fig. 8 shows the effects of using different setback distances (0, 1, 2, 3, and 4 cm) and bend angles (90°, 75°, 63°, 53°, 45°, and 33°) of the newly designed electrodes on the UI and treatment time of the raisins packed in a rectangular shape and heated to a central temperature of 52 °C using the RF system. In general, the UI reached its lowest value (0.08) when setback distance of 2 cm was used, while the highest value (0.11–0.14) was obtained when using setback distances of 0 and 4 cm. No large differences were observed when using different bend angles (90°, 75°, 63°, 53°, and 45°) at the same setback distance of 2 cm. About 4.8 min were needed to raise the central temperature of raisins from 23 °C to 52 °C using electrode configurations with a 0 cm setback distance, while more time (6.5 min) was needed when using a 4 cm setback distance.

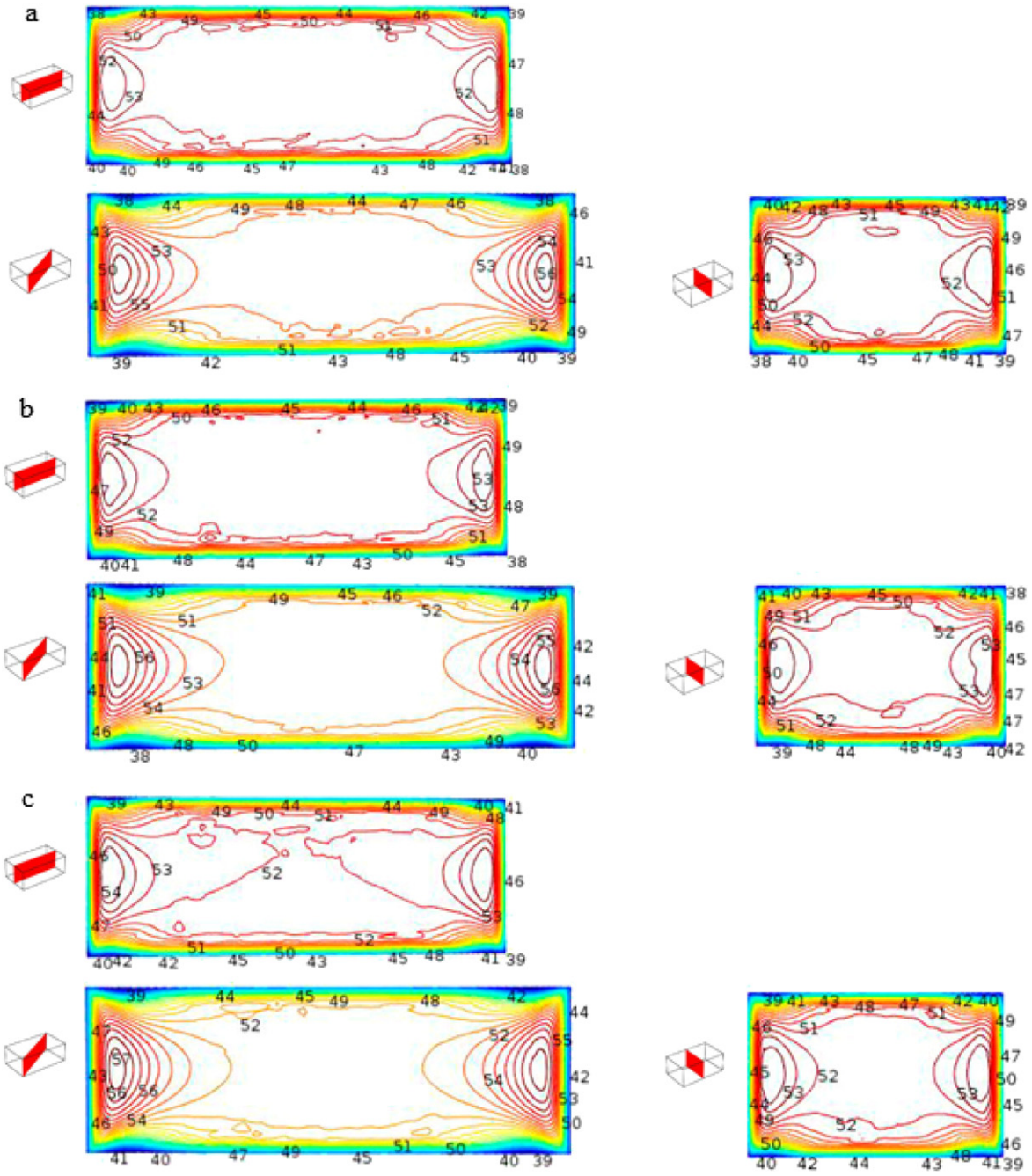

Fig. 10. Effect of different bend angles, a) 90°, b) 75°, c) 63°, d) 53°, and e) 45°, of the newly designed electrodes (setback distance 2 cm and thickness 4 cm) on the temperature distributions at three vertical layers of raisin samples packed in a rectangular shape after RF heating to a center temperature 52 °C with an electrode gap of 13.6 cm and initial temperature 23 °C (color scale is set individually for each condition).

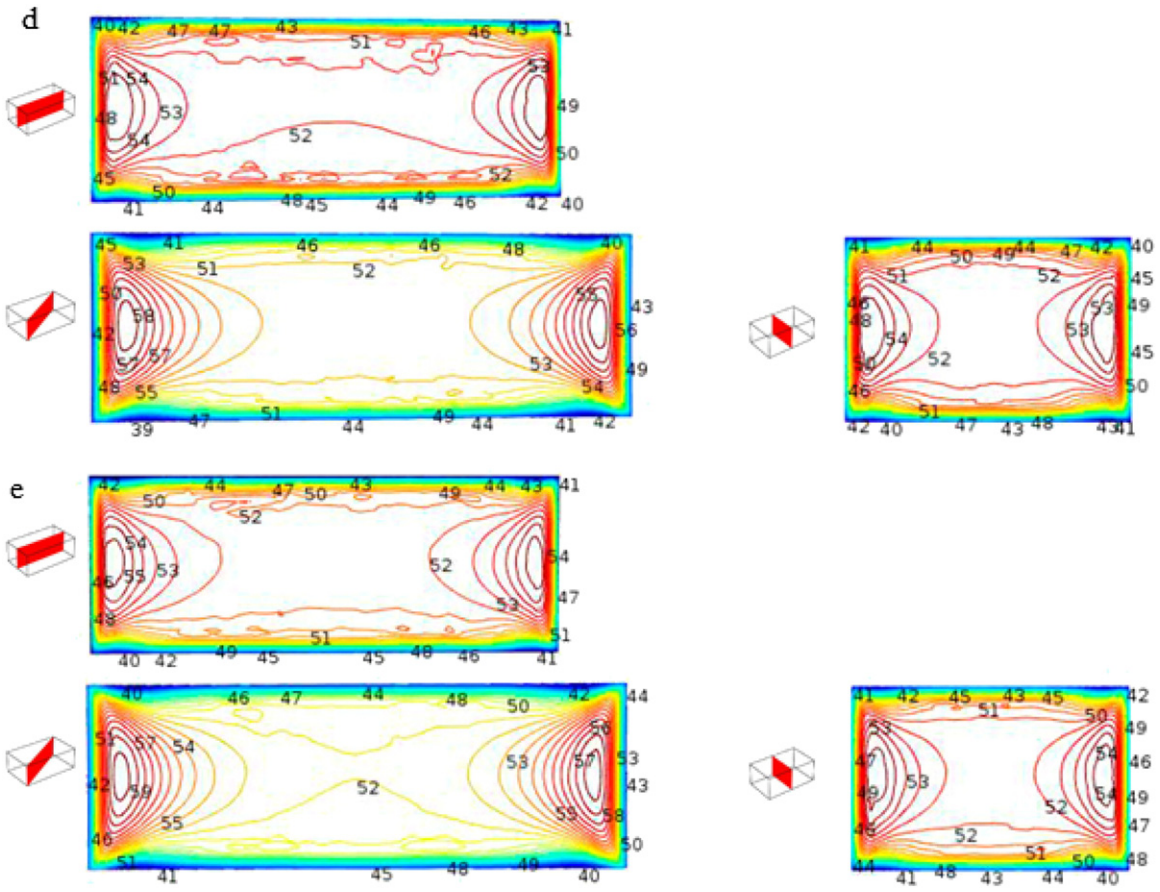

Fig. 10 (*continued*).

The large UI values obtained when using the setback distance of 0 and 4 cm were the result of the high (58, 61, and 66 °C) and low (46, 47, and 48 °C) temperatures observed in the edges and corners of three vertical layers of the rectangular sample, respectively, as explained previously and as shown in Fig. 9a and b, due to the concentration of the electromagnetic waves at these areas. When comparing the temperatures at the corners (as the highest heated area) of the sample and its center using electrode configurations with 0, 1, 2, 3, and 4 cm setback distances, the temperatures differences were 14, 9, 4, 5, and 6 °C, respectively, as shown in Fig. 9a, b, c, d, and e, which confirms that using electrodes with a setback distance of 2 cm would be an appropriate choice for improved heating uniformity.

Fig. 10a, b, c, d, and e compare the temperature distribution of raisin samples in a rectangular container in three vertical layers after being heated to a central temperature of 52 °C with an electrode gap of 13.6 cm, and using different bend angles (90°, 75°, 63°, 53°, and 45°) of the newly designed electrodes (2 cm setback distance). When reducing the bend angle of electrodes from 90° to 45°, the difference between the temperatures at the corners and center of the sample increased from 4 °C to 7 °C. This increased temperature difference indicates that using the 2 cm setback distance and 90° bend angle configuration would be the appropriate choice when designing the new electrodes for the RF system. Lower temperatures (38–40 °C) were obtained at the outer surfaces of all of the tested configurations when compared to the interior area of the samples.

3.1.3. Use of forced air (60 °C)

Effects of heating raisin samples in a rectangular geometry with different treatment conditions (forced air at 60 °C, forced air at 60 °C with, prior to, and after RF heating) to a central temperature of 55 °C using the previously determined electrode configurations (setback distance of 2 cm, bend angle of 90°, thickness of 4 cm, and gap of 13.6 cm) are presented in Fig. 11 for the temperature distributions in three vertical layers of the sample. When using forced air (60 °C), higher temperatures (60 °C) were observed in the outer surfaces, compared to 55 °C at the center of the sample (Fig. 11a). In conventional heating using forced hot air, the heat source is outside the sample. The heat is transferred from the outside to the outer surfaces of the raisins by convection, and between the raisins by conduction, until it reaches the center, a slow process. However, in RF heating, the heating occurs at the molecular level due to dipole rotation and electrical conduction mechanisms, causing the whole food to heat up at the same rate, as shown in Fig. 11b, c, and d. The difference between maximum and minimum temperatures in the raisins heated using forced air at 60 °C, and forced air at 60 °C prior to, with, and after RF heating were about 5, 27, 16, and 5 °C, respectively. It is clear from Fig. 12 that even though the UI for the samples heated by forced air at 60 °C and RF followed by forced air were comparable (0.03), only 6 min of RF heating followed by 10 min forced air at 60 °C were needed to increase the sample temperatures to >55 °C, while about 356 min were needed when using only forced air at 60 °C. Heating the samples for 10 min using forced air at 60 °C followed by

Fig. 11. Effect of different treatment conditions with forced air at 60 °C on the temperature distributions at three vertical layers of raisin samples heated in a rectangular shape to >55 °C using a) forced air at 60 °C heating, b) forced air (60 °C) followed by RF heating, c) RF heating combined with forced air (60 °C) heating, and d) RF heating followed by forced air at 60 °C heating with electrodes configuration (2 cm setback distance, 90° bend angle, and 4 cm thickness), an electrode gap 13.6 cm, and initial temperature 23 °C (color scale is set individually for each condition).

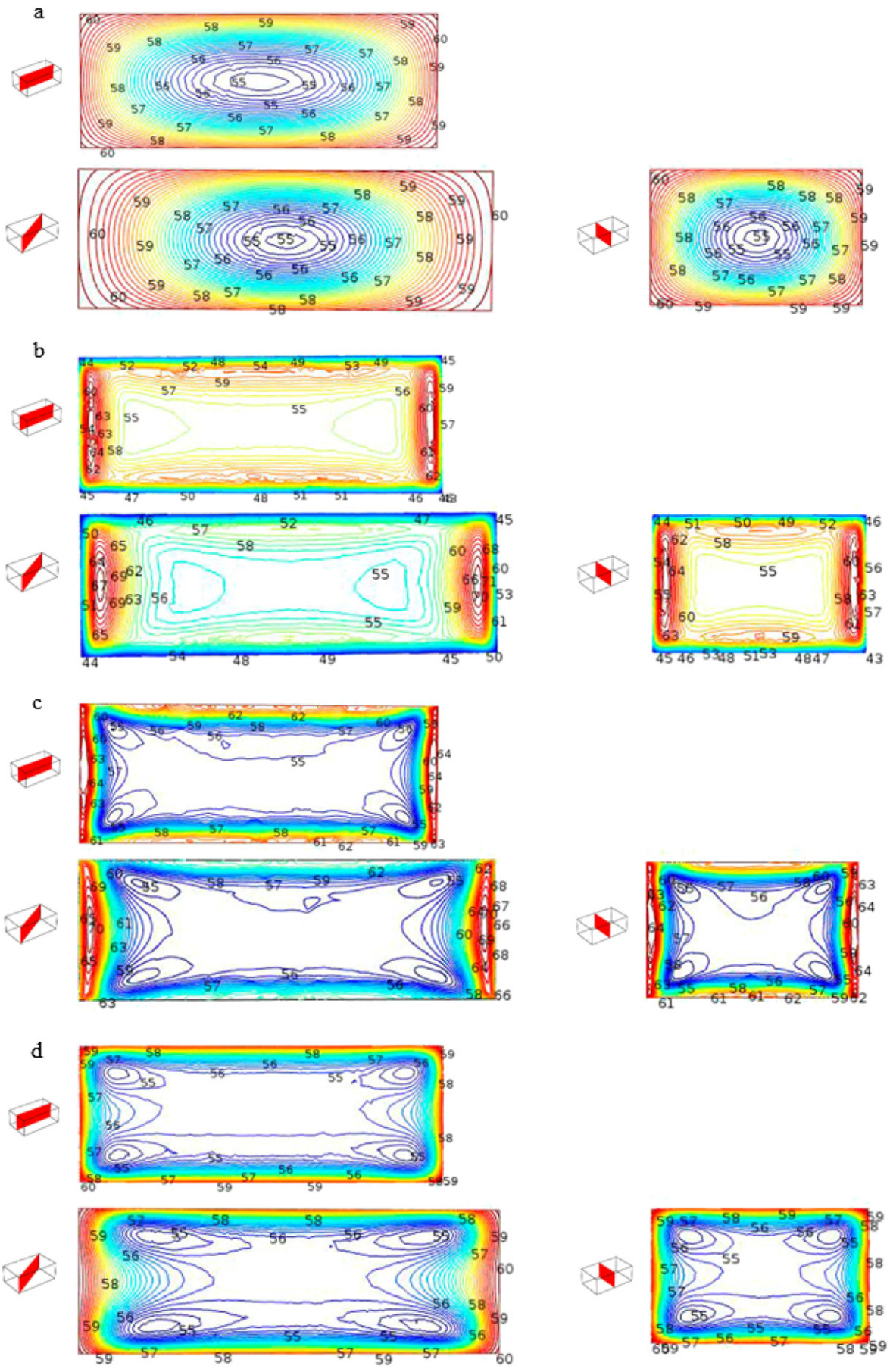
a
b
c
d

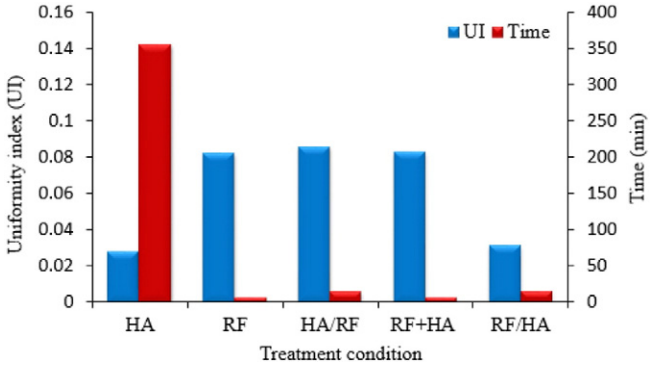

Fig. 12. Effect of different treatment combinations of RF and forced air at 60 °C on UI and treatment time of raisin samples packed in a rectangular shape and heated to central temperatures 55 °C using electrodes configuration (2 cm setback distance, 90° bend angles, and 4 cm thickness), an electrode gap 13.6 cm, and initial temperature 23 °C.

5 min RF heating raised the central temperature of the samples to 55 °C. The UI for this treatment condition was about 0.08, which indicates a poor heating uniformity due to the lower outer surfaces temperature compared to the interior area (Fig. 11b). Similar UI values were resulted when heating the samples using only RF for 6 min (center temperature of 55 °C) and when heating the samples by combined RF and forced air (60 °C).

Fig. 13 shows simulated temperature profiles of raisins heated to a central temperature of 55 °C using forced air at 60 °C and RF-forced air at 60 °C using electrode configuration with 2 cm setback distance, 90° bend angle, 4 cm thickness, and 13.6 cm gap. About 356 min were needed to increase the central temperature of raisins from about 23 °C to 55 °C using forced air at 60 °C. In comparison, only 6 min of RF-forced air heating were needed for raisin samples to reach a central temperature of 55 °C.

4. Conclusions

Effects of package geometries, electrode configuration, and a supplemental heat treatment with forced air at 60 °C were investigated on the RF heating uniformity of bulk raisins. Overheating at the edges and corners of the raisins treated in rectangular and cylindrical shaped containers was observed with a difference of about 36 °C and 24 °C throughout the sample, respectively. The simulated temperature distribution and heating uniformity of RF treated raisins was significantly improved when containers with rounded edges and corners were used, with a difference of about 12 °C. Using RF heating with a 2 cm setback distance and 90° bend angle of the newly designed electrodes, followed by forced air at 60 °C also improved the heating uniformity with a difference of about 5 °C. The time required to heat the raisins from 23 °C to the lethal target temperature, 55 °C, was reduced significantly from 356 min for forced air heating alone, to only 16 min using RF heating followed by forced air at 60 °C for rectangular containers. Treatment protocol to disinfest insects in dried fruits can be developed based upon this simulation method.

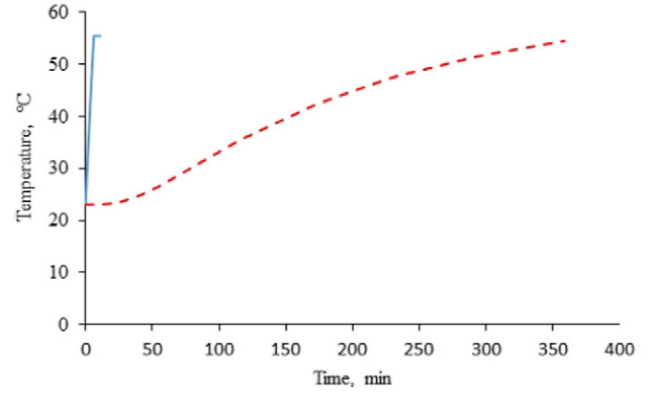

Fig. 13. Simulated temperature-time histories of raisin samples packed in a rectangular container and heated to a center temperature 55 °C using forced air at 60 °C (- - -) and RF heating followed by forced air at 60 °C heating (—) with electrodes configuration (2 cm setback distance, bend angle 90°, thickness 4 cm, and gap 13.6 cm).

Acknowledgements

The authors acknowledge the financial support from the Agricultural Research Center at King Saud University, Riyadh, Saudi Arabia and the Agricultural Research Center at Washington State University, Pullman, USA.

References

Alfaifi, B., Tang, J., Jiao, Y., Wang, S., Rasco, B., Jiao, S., & Sablani, S. (2014). Radio frequency disinfestation treatments for dried fruit: Model development and validation. *J. Food Eng., 120*, 268–276.

Alfaifi, B., Wang, S., Tang, J., Rasco, B., Sablani, S., & Jiao, Y. (2013). Radio frequency disinfestation treatments for dried fruits: Dielectric properties. *LWT Food Sci. Technol., 50*(2), 746–754.

Barber, H. (1983). *Electroheat* (1st ed.). London, UK: Granada Publishing Limited.

Birla, S. L., Wang, S., & Tang, J. (2008). Computer simulation of radio frequency heating of model fruit immersed in water. *J. Food Eng., 84*(2), 270–280.

Birla, S. L., Wang, S., Tang, J., & Hallman, G. (2004). Improving heating uniformity of fresh fruits in radio frequency treatments for pest control. *Postharvest Biol. Technol., 33*(2), 205–217.

Chen, L., Wang, K., Li, W., & Wang, S. (2015). A strategy to simulate radio frequency heating under mixing conditions. *Comput. Electron. Agric., 118*, 100–110.

COMSOL Material Library (2012). *COMSOL multiphysics, V4.2a.* MA, USA: Burlington.

Datta, A. K., & Zhang, H. (2001). Electromagnetics of microwave heating: Magnitude and uniformity of energy absorption in an oven. In A. K. Datta, & R. C. Anantheswaran (Eds.), *Handbook of microwave technology for food applications* (pp. 33–68). New York, USA: Marcel Dekker, Inc.

Fu, Y. C. (2004). Fundamentals and industrial applications of microwave and radio frequency in food processing. In J. S. Smith, & Y. H. Hui (Eds.), *Food processing: Principles and applications* (pp. 79–100). Iowa: Blackwell.

Ha, J. W., Kim, S. Y., Ryu, S. R., & Kang, D. H. (2013). Inactivation of *Salmonella enterica* serovar typhimurium and *Escherichia coli* O157:H7 in peanut butter cracker sandwiches by radio-frequency heating. *Food Microbiol., 34*(1), 145–150.

Hadjinicolaou, J. (1931). Effect of certain radio waves on insects affect certain stored products. *Journal of the New York Entomological Society, 39*(2), 145–150.

Hansen, J. D., Drake, S. R., Watkins, M. A., Heidt, M. L., Anderson, P. A., & Tang, J. (2006). Radio frequency pulse application for heating uniformity in postharvest codling moth (Lepidoptera: Tortricidae) control of fresh apples (*Malus domestica* Borkh). *J. Food Qual., 29*(5), 492–504.

Harraz, H. (2007). *Radio frequency heating for dehydration and pest control of in-shell peanuts.* (Master of Sciences Thesis) Auburn, AL: Auburn University.

Headlee, T. J., & Burdette, R. C. (1929). Some facts relative to the effect of high frequency radio waves on insect activity. *Journal of the New York Entomological Society, 37*(1), 59–64.

Huang, Z., Marra, F., & Wang, S. (2016). A novel strategy for improving radio frequency heating uniformity of dry food products using computational modeling. *Innovative Food Sci. Emerg. Technol., 34*, 100–111.

Huang, Z., Zhang, B., Marra, F., & Wang, S. (2016). Computational modelling of the impact of polystyrene containers on radio frequency heating uniformity improvement for dried soybeans. *Innovative Food Sci. Emerg. Technol., 33*, 365–380.

Ikediala, J. N., Hansen, J., Tang, J., Drake, S. R., & Wang, S. (2002). Development of a saline water immersion technique with RF energy as a postharvest treatment against codling moth in cherries. *Postharvest Biol. Technol., 24*(1), 25–37.

Jeong, S. G., & Kang, D. H. (2014). Influence of moisture content on inactivation of *Escherichia coli* 0157:H7 and *Salmonella enterica* serovar typhimurium in powdered red and black pepper spices by radio-frequency heating. *Int. J. Food Microbiol., 176*, 15–22.

Jiao, S., Johnson, J. A., Tang, J., & Wang, S. (2012). Industrial-scale radio frequency treatments for insect control in lentils. *J. Stored Prod. Res., 48*, 143–148.

Jiao, Y., Tang, J., & Wang, S. (2014). A new strategy to improve heating uniformity of low moisture foods in radio frequency treatment for pathogen control. *J. Food Eng., 141*, 128–138.

Ling, B., Hou, L., Li, R., & Wang, S. (2016). Storage stability of pistachios as influenced by radio frequency treatments for postharvest disinfestations. *Innovative Food Sci. Emerg. Technol., 33*, 357–364.

Lutz, F. E. (1927). A much abused but still cheerful cricket. *Journal of the New York Entomological Society, 35*(3), 307–308.

Marra, F., Lyng, J., Romano, V., & McKenna, B. (2007). Radio-frequency heating of foodstuff: Solution and validation of a mathematical model. *J. Food Eng., 79*(3), 998–1006.

Metaxas, A. C. (1996). *Foundations of electroheat—A unified approach* (1st ed). New York, USA: John Wiley & Sons.

Ramaswamy, H., & Tang, J. (2008). Microwave and radio frequency heating. *Food Sci. Technol. Int., 14*(5), 423–427.

Sosa-Morales, M. E., Tiwari, G., Wang, S., Tang, J., Lopez-Malo, A., & Garcia, H. S. (2009). Dielectric heating as a potential post-harvest treatment of disinfesting mangoes. II: Development of RF-based protocols and quality evaluation of treated fruits. *Biosyst. Eng.*, *103*(3), 287–296.

Tiwari, G., Wang, S., Birla, S. L., & Tang, J. (2008). Effect of water assisted radio frequency heat treatment on the quality of 'Fuyu' persimmons. *Biosyst. Eng.*, *100*(2), 227–234.

Tiwari, G., Wang, S., Tang, J., & Birla, S. L. (2011a). Analysis of radio frequency (RF) power distribution in dry food materials. *J. Food Eng.*, *104*(4), 548–556.

Tiwari, G., Wang, S., Tang, J., & Birla, S. L. (2011b). Computer simulation model development and validation of radio frequency (RF) heating of dry food materials. *J. Food Eng.*, *105*(1), 48–55.

Uyar, R., Bedane, T. F., Erdogdu, F., Palazoglu, T. K., Farag, K. W., & Marra, F. (2015). Radio frequency thawing of food products—A computational study. *J. Food Eng.*, *146*, 163–171.

Wang, S., Birla, S. L., Tang, J., & Hansen, J. D. (2006). Postharvest treatment to control codling moth in fresh apples using water assisted radio frequency heating. *Postharvest Biol. Technol.*, *40*(1), 89–96.

Wang, S., Ikediala, J. N., Tang, J., Hansen, J. D., Mitcham, E., Mao, R., & Swanson, B. (2001). Radio frequency treatments to control codling moth in in-shell walnuts. *Postharvest Biol. Technol.*, *22*(1), 29–38.

Wang, S., Tang, J., & Hansen, J. D. (2007). Experimental and simulation methods of insect thermal death kinetics. In J. Tang, E. Mitcham, S. Wang, & S. Lurie (Eds.), *Heat treatments for postharvest pest control: Theory and practice* (pp. 105–132). Oxon, UK: CABI Publishing.

Wang, S., Tiwari, G., Jiao, S., Johnson, J. A., & Tang, J. (2010). Developing postharvest disinfestation treatments for legumes using radio frequency energy. *Biosyst. Eng.*, *105*(3), 341–349.

Zhou, L., & Wang, S. (2016). Verification of radio frequency heating uniformity and *Sitophilus oryzae* control in rough, brown, and milled rice. *J. Stored Prod. Res.*, *65*, 40–47.

Zhou, L., Ling, B., Zheng, A., Zhang, B., & Wang, S. (2015). Developing radio frequency technology for postharvest insect control in milled rice. *J. Stored Prod. Res.*, *62*, 22–31.